Thermoresponsive mesoporous silica nanoparticles as a carrier for skin delivery of quercetin

Research Paper

Thermoresponsive mesoporous silica nanoparticles as a carrier for skin delivery of quercetin

Elena Ugazio[a,d,e], Lucia Gastaldi[a], Valentina Brunella[b,d], Dominique Scalarone[b,d], Sushilkumar A. Jadhav[b,d], Simonetta Oliaro-Bosso[a,e], Daniele Zonari[a], Gloria Berlier[b,d], Ivana Miletto[c] and Simona Sapino[a,d,e*]

[a]*Università di Torino, Dipartimento di Scienza e Tecnologia del Farmaco, Via P. Giuria 9, 10125 Torino, Italy.*

[b]*Università di Torino, Dipartimento di Chimica, Via P. Giuria 7, 10125 Torino, Italy.*

[c]*Università del Piemonte Orientale, Dipartimento di Scienze e Innovazione Tecnologica, Viale T. Michel 11, 15121, Alessandria, Italy*

[d]*NIS (Nanostructured Interfaces and Surfaces) Centre, Università di Torino, Italy.*

[e]*"G. Scansetti" Interdepartmental Centre, Università di Torino, Italy.*

**Corresponding author: Tel: +39 0116707192; Fax: +39 0116707687*

E-mail address: simona.sapino@unito.it

Keywords:

PNIPAM, copolymer, MCM-41, biocompatibility, antioxidant, controlled release, cutaneous application

Abstract

Recently, mesoporous silica nanoparticles (MSNs) have emerged as promising drug delivery systems able to preserve the integrity of the carried substance and/or to selectively reach a target site, anyway they have rarely been explored for skin application. In this study, thermoresponsive MSNs, designed to work at physiologic cutaneous temperature, are proposed as innovative topical carriers for quercetin (Q), a well-known antioxidant. The thermosensitive nanoparticles were prepared by functionalizing two different types of matrices, with pore size of 3.5 nm (MSN_{small}) and 5.0 nm (MSN_{big}) respectively, carrying out a free radical copolymerization of N-isopropylacrylamide (NIPAM) and 3-(trimethoxysilyl)propyl methacrylate (MPS) inside the mesopores. The obtained copolymer-grafted MSNs (copoly-MSNs) were physico-chemical characterized and their biocompatibility was attested on a human keratinocyte cell line (HaCaT). The release profiles were assessed and the functional activity of Q, free or loaded, was evaluated in terms of antiradical and metal chelating activities. *Ex vivo* accumulation and permeation through porcine skin were also investigated. The characterization confirmed the copolymer functionalization of the MSNs. In addition, both the bare and functionalized silica matrices were found to be biocompatible. Among the copolymer-grafted complexes, Q/copoly-MSN_{big} exhibited more evident thermoresponsive behavior proving the potential of these thermosensitive systems for advanced dermal delivery.

1. Introduction

The biological role of flavonoids, a large class of secondary plant metabolites, is well established. Flavonoids are abundantly present in fruit, vegetable, cocoa, wine, tea, and soy. They share a common carbon skeleton of two benzene rings joined by a 3-carbon bridge (C6–C3–C6), comprising many subclasses, such as flavonols, flavones, anthocyanidins, flavanones, and isoflavones (Middleton et al., 2000; Miyake and Shibamoto, 1997). Flavonoids are helpful in the treatment of many diseases and are important antioxidant, anticancer and neuroprotective agents (Maalik et al., 2014). Notably, they have been proposed as an interesting cost-effective therapeutic tool in inflammatory diseases and represent an alternative to immunosuppressive agents, which are known to have multiple side effects (Ribeiro et al., 2015). In addition flavonoids, besides being efficient free radical scavengers (Roubalova et al., 2015), can up-regulate the endogenous antioxidant system (Ehren and Maher, 2013), suppress oxidative and nitrosative stress, decrease macrophage oxidative stress through cellular oxygenase inhibition as well as through interaction with several signal transduction pathways. Moreover, they also show therapeutic effects against atherosclerosis (Siasos et al., 2013).

Interestingly, several studies have demonstrated the efficacy of flavonoids in reducing the symptoms of chronic venous insufficiency. Indeed, flavonoids have been widely used to manage the symptoms of venous diseases because they can address certain microcirculatory deficiencies involved in ulcer pathophysiology (Rabe et al., 2015). These include decreasing leukocyte adhesion and free radical formation, decreasing permeability and fragility of vein valves and venous wall (and therefore decreasing abnormal leakage in the lower limbs), and increasing venous flow (Werner et al., 2015). Nevertheless, they cannot attack the underlying cause of venous hypertension (Scallon et al., 2013).

Most flavonoids are administered orally, but they can also be applied topically in the form of creams, gels, lotions, etc. The topical use of flavonoids is very desirable since it allows a synergic combination of three important benefits: the skin hydration of the affected area, the massage action that takes place

during the application, the active compound release. Accordingly, flavonoid extract, having antioxidant, anti-inflammatory and sun protection properties, can enrich skin care products, adding valuable benefits to the formulation (Saija et al., 1998).

Cutaneous application of flavonoids, however, is limited by their low solubility, low stability and low release after application (Kim et al., 2004; Kumar and Pandey, 2013). Moreover, flavonoid chemical changes resulting from degradation may decrease the effectiveness and safety of skin care products. Thus, to ensure that topically administered antioxidants are effective upon skin application, a crucial point in the product formulation is its stabilization. Under this point of view, antioxidants are very unstable and they may be converted to an inactive form before reaching the target; on the other hand, antioxidants must be properly adsorbed into the skin, reach their target tissue in the active form and remain there long enough to exert the desired effects.

Taking into account these considerations, we designed a thermoresponsive delivery system able to release bioactive compounds when in contact with the skin.

Recently, MSNs have been proposed in the dermocosmetic field as carriers of active ingredients (Ambrogi et al., 2007; Berlier et al., 2013a; Gastaldi et al., 2012; Sapino et al., 2015). They are characterized by an ordered mesoporous structure and high biocompatibility; moreover, by grafting functional moieties on their surface, it is possible to modulate the delivery of a bioactive agent in response to different *stimuli* including light, temperature, pH, electric fields, or chemicals (e.g. enzymes). Functional moieties used for this purpose are often smart polymers which can protect the drug until it reaches the site of action and can then modulate its release to obtain the desired release profile (Wang, 2009).

Smart polymers are materials responding in a fast and substantial way to very slight changes in the environment. Poly(*N*-isopropylacrylamide) (PNIPAM) is a temperature-responsive polymer that was first synthesized in the 1950s (Schild, 1992). At approximately 33 °C, it exhibits a lower critical solution

temperature (LCST). Above this temperature, the swollen hydrated polymer chains shrink to dehydrated ones, losing about 90% of their total mass. As this coil-to-globule transition occurs at a temperature close to human body temperature, PNIPAM has recently been proposed as a smart polymeric carrier suitable to deliver therapeutic molecules (Gandhi et al., 2015; Natalia et al., 2015). Generally, to be of interest for potential *in vivo* applications, carriers must retain active molecules tightly before usage, but they have to release them in the application site according to individual requirements. Recently, variable stimuli-responsive systems based on MSNs have been designed for drug delivery. However, to date, very few reports have focused on the controlled dermal release of active substances, while most research and development activities are aimed at encapsulating drugs for systemic applications.

Thus, in order maintain the effectiveness of antioxidants in skin care products during shelf-life and the period-after-opening, we developed MSNs functionalized with a thermoresponsive copolymer of NIPAM and we successfully loaded them with the flavonoid quercetin as a model compound characterized by poor water solubility, low stability and a short half-life (Berlier et al., 2013b; Li et al., 2013). Taking advantage of the attractive tunable structural features of MSNs, nanoparticles with two different pore sizes (3.5 and 5.0 nm) were synthesized in the attempt to find the best affinity for the guest molecule.

After a physico-chemical characterization and a biocompatibility test of these delivery systems, preliminary experiments were performed to verify their capability of triggering the flavonoid release upon skin contact. Hence, the antioxidant efficacy of the most promising complexes was assessed by *in vitro* studies and the permeation and accumulation of quercetin through the skin were tested by Franz diffusion cells.

This proof-of-concept study is expected to address the challenges related to the application of copolymer-functionalized MSNs as carriers for the loading and thermosensitive release of active molecules on the skin.

2. Materials and methods

2.1. Materials

3,3′,4′,5,7-Pentahydroxyflavone (quercetin anhydrous, Q), 1,3,5-trimethylbenzene (TMB), 2,2′-azobis(2-methylpropionitrile) 98% (AIBN), 3-(trimethoxysilyl)propyl methacrylate (MPS), N-isopropylacrylamide (NIPAM), absolute ethanol, dimethyl sulfoxide (DMSO), hexadecyltrimethylammonium bromide (CTAB), methanol, tetraethyl orthosilicate (TEOS), sodium phosphate dibasic, 3-(2-Pyridyl)-5,6-diphenyl-1,2,4-triazine-*p,p′*-disulfonic acid monosodium salt hydrate (ferrozine), iron(II) sulfate hydrate ($FeSO_4$), sodium azide, sulforhodamine B (SRB), Dulbecco's modified Eagle's medium (DMEM), fetal calf serum, Tris buffered saline, trichloroacetic acid and antibiotics for cell cultures were purchased from Sigma–Aldrich. Acetic acid was from Carlo Erba. Sodium chloride, hydroxyethylcellulose (HEC) and propylene glycol were purchased from ACEF. Potassium dihydrogen phosphate dehydrate and sodium hydroxide were from Fluka. Human immortalized keratinocyte cell line, HaCaT, was kindly provided by Dr. Carlotta Castagnoli (Dipartimento di Chirurgia Generale e Specialistiche, Banca della Cute, AOU Città della Salute e della Scienza di Torino, Italy).

2.2. Synthesis of MSNs

MCM-41-like nanoparticles were synthesized by optimizing a literature procedure, employing CTAB as the structure directing agent (SDA) and TEOS as the silica source (Kresge et al., 1992). In particular, two types of MSNs were prepared: conventional MSNs with small pore size (i.e. 3.5 nm) and MSNs with big pore size (i.e. 5.0 nm), hereafter labelled MSN_{small} and MSN_{big}, respectively.

In a typical reaction to obtain MSN_{small}, CTAB (1 g) was dissolved in distilled water (480 mL); the solution was heated at 80 °C and then NaOH (3.5 mL, 2 M) was added, so the mixture was stirred for 30 min. TEOS (5 mL) was added dropwise. The mixture was then stirred for 2 h at 80 °C. After cooling to

room temperature (RT), the powder product was isolated by filtration, washed with distilled water (750 mL) and methanol (500 mL), and air-dried for 24 h.

The synthesis of MSN_{big} was obtained employing 1,3,5-trimethylbenzene (TMB) as the micelle core swelling agent. In particular, in this case, differently from MSN_{small} synthesis, after NaOH addition and the stabilization of the temperature, a proper amount of TMB was added to the system. The mixture was stirred for 30 min for the formation of a stable white emulsion. Then TEOS was added following the same procedure as reported for MSN_{small}.

In both cases, the as-synthesized materials were calcined by flowing nitrogen from RT to 550 °C (2 °C/min ramp) and then switching the flow to oxygen, for a 6 h isotherm at 550 °C.

2.3. Synthesis of copolymer-grafted MSNs

Functionalized MSNs were obtained by carrying out the free radical copolymerization of NIPAM and MPS (poly(NIPAM-co-MPS)) inside the mesopores of MCM-41-like nanoparticles, after infiltration of monomers and AIBN initiator into the mesopores. Stable anchoring of the copolymer chains is provided by condensation of trimethoxysilane groups of MPS with silanols on the silica surface (Brunella et al., 2016). In a typical reaction, MSNs (280 mg) were dispersed by sonication at RT in 10 mL of ethanol solution of NIPAM (70 mg, 0.62 mmol) and AIBN (3.39 mg, 0.02 mmol). After 30 min, MPS (7.68 mg, 0.03 mmol) was added into the suspension and dispersed evenly by sonication for another 30 min. The dispersion was injected in a three neck round bottom flask equipped with condenser and nitrogen inlet. The injected suspension was then heated at 70 °C under nitrogen for 16 h. The product was dried by nitrogen flow, washed three times with deionized water and recovered by centrifugation. The resultant functionalized nanoparticles are hereafter labeled: copoly-MSN_{small} and copoly-MSN_{big}.

2.4. Quercetin loading

Q loading in nanoparticles with different pore sizes was performed by impregnation in DMSO, soaking a fixed amount of MSNs (MSN_{small}, MSN_{big}, copoly-MSN_{small}, copoly-MSN_{big}) in a concentrated solution of Q.

Firstly, Q solution (2 mL) in DMSO (15 mg/mL) was prepared; after leaving the solution under magnetic stirring in the dark for few minutes, an aliquot of silica nanoparticles (bare or functionalized MSNs) was added, in 1/1 weight ratio with respect to Q. The solution was magnetically stirred in the dark for 24 h at 40 (± 0.5) °C in a FTC901 cooled incubator (VELP Scientifica). Distilled water (18 mL) was then added to obtain the precipitation of the complex. The suspension was centrifuged at 19000 × *g* for 15 min at 20 (± 0.5) °C, then the precipitate was firstly washed with 2 mL of methanol, secondly with 2 mL of distilled water and then centrifuged. After centrifugation, the precipitate was dried under *vacuum*. The resulting complexes are hereafter labelled as Q/MSN_{small}, Q/MSN_{big}, Q/copoly-MSN_{small}, Q/copoly-MSN_{big}.

2.5. Quercetin analysis and loading evaluation

UV–Vis spectrophotometry calibration curves were obtained in different media with diluted Q solutions over the range 1.0 - 5.0 × 10^{-5} M by using a DU 730 UV/Vis Spectrophotometer (Beckmann Coulter). The molar extinction coefficient (ε) was 20168 M^{-1} (R^2 = 0.9932) in DMSO and 19088 M^{-1} (R^2 = 0.9958) in DMSO/phosphate buffer pH 6.5 (25/75 v/v) mixture, respectively.

HPLC analysis was performed by an apparatus consisting of a PU-1580 pump unit control (Jasco), a UV-1575 UV–Vis detector (Jasco), a CBM-10A integrator (Shimadzu) and a RP-C18 column (Purospher STAR RP-18 endcapped, 150 × 4.6 mm; 5 μm); mobile phase: methanol/water/acetic acid (50/47/3 v/v/v), flow rate: 0.8 mL/min. The elution profile was monitored at 370 nm (retention time around 8.5 min). The amount of Q in the samples was quantified using the standard curve generated by calculating the HPLC peak area of pure Q (in ethanol ε was 312328 M^{-1}; R^2 = 0.9991).

The spectrophotometric evaluation of loaded Q was carried out by dispersing 1.5-2.0 mg of each complex into DMSO (10.0 mL) with stirring at 40 °C in darkness for 24 h. After centrifugation at 19000 × g for 15 min, the supernatant was spectrophotometrically analyzed and the loading content (% Q) was calculated according to Eq. (1):

$$\%Q = \frac{amount\ of Q\ in\ the\ complex}{total\ amount\ of\ the\ complex} \times 100 \quad (1)$$

2.6. Physico-chemical characterization

2.6.1. High resolution transmission electron microscopy

High resolution transmission electron microscopy (HRTEM) observations were performed by a JEM 3010 instrument (JEOL) operating at 300 kV. For specimen preparation powdery samples were supported onto perforated carbon coated copper grids by dry deposition.

2.6.2. Gas–volumetric analysis

Specific surface area (SSA), pore volume and size were measured by gas–volumetric analysis (N_2 adsorption–desorption isotherms at liquid nitrogen temperature, LNT) using an ASAP 2020 physisorption analyzer (Micromeritics). SSA and average pore size were calculated by the Brunauer–Emmet–Teller (BET) and the Barrett–Joyner–Halenda (BJH) methods, respectively. For the latter, the Kruk–Jaroniec–Sayari (KJS) equations were employed in the adsorption isotherms. Prior to analyses, the samples were outgassed overnight at RT.

2.6.3. Thermogravimetric analysis

Thermogravimetric analysis (TGA) was carried out with a TA Q500 model from TA Instruments by heating samples at a rate of 10 °C/min in nitrogen from 50 to 600 °C and in air from 600 to 800 °C.

2.6.4. Mean diameter and ζ potential measurements

Mesoporous nanoparticles were characterized in terms of average diameter and polydispersity using the dynamic light scattering technique (DLS) (90 Plus Particle Size Analyzer, Brookhaven Instruments) at the fixed angle of 90°. ζ potential of each sample was calculated by electrophoretic measurements using the ZetaPlus-Zeta Potential Analyzer (Brookhaven Instruments). All the samples were previously suspended in ultra-filtered water (0.1% w/v), without altering the pH of the dispersion medium, sonicated for about 10 min and then analyzed at 25 ± 0.1 °C.

2.7. Biocompatibility of the silica matrices

The biocompatibility of the silica matrices was evaluated by monitoring the viability of human keratinocyte cell line (HaCaT) by sulforhodamine B colorimetric proliferation assay (SRB assay) (Skehan et al., 1990), modified by Vichai and Kirtikara (Vichai and Kirtikara, 2006).

HaCaT cells were routinely grown in DMEM added with 10% (v/v) fetal calf serum, 1% (v/v) penicillin–streptomycin, and maintained in standard conditions (37 °C, 5% CO_2 and 95% humidity). The SRB proliferation assays in the presence of 0.291, 2.91, 8.75, 17.5 ($\times 10^{-3}$) mg/mL of the silica matrices (MSN_{big}, copoly-MSN_{big}, MSN_{small} and copoly-MSN_{small}) pre-suspended in culture medium containing 1% (v/v) ethanol was carried out as previously described (Sapino et al., 2015). The experiment was replicated twice under unchanged conditions.

2.8. Testing of quercetin/MSNs complex properties

2.8.1. Quercetin release tests

A weighted amount of each prepared complex was dispersed in 25 mL of phosphate buffer (pH 6.5)/DMSO (75/25 v/v) mixture. The obtained dispersions were placed in incubator at 20 °C (below LCST) and 40 °C (above LCST). At each predetermined time interval, 1.0 mL aliquots of the dispersions

were withdrawn and replaced with fresh release medium. After centrifugation at 16000 × *g* for 10 min, the concentrations of Q in the supernatant were determined *via* UV–visible spectroscopy by monitoring absorption at λ_{max} = 376 nm. The results of the release tests are expressed as percentage of Q released over time.

2.8.2. Antioxidant activity (DPPH• assay)

DPPH• scavenging activity was determined according to the method already reported in a previous work (Berlier et al., 2013a). Firstly, a calibration curve was obtained, then an appropriate sample volume was added to a solution of DPPH• radical and the spectrophotometric analysis was performed after the reaction reached a plateau. Briefly, dilutions (100.0 µL) of Q, free or immobilized in MSN_{big} or in copoly-MSN_{big}, in the range 10.0–250.0 µM, were added to 5.0 mL of a saturated solution of DPPH• in ethanol/water (50/50 v/v) mixture. Samples were kept under magnetic stirring for 10 min at RT in darkness to reach the steady-state condition and then centrifuged. Finally, the absorbance was read spectrophotometrically at 525 nm.

For each tested sample, the inhibition percentage of DPPH• at the steady-state was determined as described in Eq. (2):

$$\% \text{ RSA} = (Abs_{blank}\text{-}Abs_{sample}/Abs_{blank}) \times 100 \quad (2)$$

These percentages were plotted vs. the concentration of Q contained in the samples. Experiments were carried out in triplicate.

2.8.3 Metal chelating effect (Fe^{2+}-Ferrozine assay)

The ability of Q, Q/MSN_{big} or Q/copoly-MSN_{big} to chelate ferrous ions (Fe^{2+}) was investigated by following the method previously described (Berlier et al., 2013a). Different concentrations of free or complexed antioxidant (25–50 µM) in 4.0 mL ethanol/water (20/80 v/v) solution were incubated with 50

μL of $FeSO_4$ (2.0 mM) aqueous solution under magnetic stirring for 20 min. An aliquot (200 μL) of ferrozine aqueous solution (2.0 mM) was then added. After the mixtures had reached equilibrium (7 min of magnetic stirring, RT), they were centrifuged and then spectrophotometrically analyzed at 562 nm. Experiments were carried out in triplicate.

The ability of each antioxidant sample to inhibit the formation of the ferrous–ferrozine complex, expressed as its metal chelating effect (% MCE), was then calculated and plotted using Eq. (3):

$$\% \text{ MCE} = (Abs_{blank}\text{-}Abs_{sample}/Abs_{blank}) \times 100 \quad (3)$$

2.8.4. Ex vivo experiments on porcine skin

For the e*x vivo* experiments on porcine skin, a hydrogel was prepared by simply mixing 2.0 g of HEC with 73.0 mL of distilled water at about 80 °C. The resulting solution was mechanically stirred by a DLS stirrer (Velp Scientifica) until a gel was obtained. When RT was reached, 20.0 g of propylene glycol containing a proper amount of Q or Q complex and 5.0 g of ethanol were added, then the mixture was stirred until a homogeneous gel was obtained.

Transepidermal permeation and skin uptake were determined using vertical Franz cells and porcine skin. Skin slices were isolated with an Acculan dermatome (Aesculap) from outer side of pig ears freshly obtained from a local slaughterhouse and then stored for at least 24 h at −18 °C. Prior to each experiment, the excised skin was rinsed with normal saline solution and pre-hydrated by floating it in 0.002% (w/v) sodium azide aqueous solution. The skin was then sandwiched between the two cells with the *stratum corneum* side upwards. The receptor chamber was filled with 4.0 mL of normal saline solution/ethanol (80/20 v/v) mixture. Test formulations, consisting of free or immobilized Q, dispersed into 2.0 g of hydrogel, were applied to the skin surface (available diffusion area of 0.65 cm^2) at the 1.0% w/w concentration. During the experiment, Franz cells were maintained at controlled temperature of 35 ± 1 °C and the receptor chamber was continuously stirred. After 24 h, the content of the receptor chamber was

removed and Q permeation was determined by HPLC analysis. Afterwards, the application site of the skin was washed with normal saline solution. The skin was then cut with a scalpel into small pieces and added to 2.0 mL of ethanol/DMSO (90/10 v/v) mixture for Q extraction. After 20 h of magnetic stirring at RT, the resulting suspensions were sonicated in an ETH2200 ultrasonic water bath (Soltec) for 15 min, then centrifuged and the supernatants were analyzed by HPLC. The skin uptake was expressed as μg Q/cm^2 skin diffusion area. Experiments were carried out in triplicate and a placebo formulation was used as control.

3. Results and discussion

3.1. Physico-chemical characterization

In a previous work, we already studied the applicability of MSNs with an average pore size of 3.5 nm (MSN_{small}) as matrices for dermal delivery of Q, and the physico-chemical properties of the bare nanoparticles, investigated by TEM, XRD and BET analyses, were extensively discussed (Sapino et al., 2015).

In this research, MSNs with an average pore diameter of 5.0 nm (MSN_{big}) were synthesized by suitable modification of the standard synthesis by using TMB as micelle core-swelling agent to increase the diameter of the pores. One-step post-synthesis grafting of thermoresponsive poly(NIPAM-co-MPS) on the nanoparticles was successfully carried out following the same procedure already reported elsewhere (Brunella et al., 2016).

For sake of brevity, here only a brief description of the physico-chemical properties of the different MSNs used as Q delivery systems is given. We suggest referring to our recent papers for a more detailed characterization of MSN_{small} and MSN_{big}, both bare and copolymer-grafted.

The HRTEM images of MSN_{big}, like those of MSN_{small} (here not shown), revealed the presence of nanosized mesoporous spherical particles, with an average particle size of ca. 100-150 nm, characterized

by regular and ordered channels with hexagonal symmetry (Fig. 1). Moreover, TEM analysis confirmed that the copolymer-grafting procedure did not affect the mesoporous structure and the morphology of the MSNs (Jadhav et al., 2015).

The XRD patterns of the two bare samples, MSN_{small} and MSN_{big}, do not differ significantly and show the (100) peak and the well-separated (110) (200) reflections proving that both samples have pores in a hexagonal setting with a high degree of structural order, typical of the MCM-41-like structure. Notably, such order is maintained also after the copolymer grafting, indicating that the ordered structure of the silica particles is preserved under the applied grafting conditions (Jadhav et al., 2015).

The low temperature adsorption-desorption isotherm of both parent nanoparticles (MSN_{small} and MSN_{big}) presents a type IV isotherm typical of a mesoporous matrix. For each matrix, specific surface area, cumulative pore volume and mean pore diameter were calculated before and after the grafting procedure (Brunella et al., 2016; Jadhav et al., 2015). As summarized in Table 1, pore diameter and accessible pore volume were reduced by the co-polymer grafting thus proving that in both types of functionalized MSNs, the volume available inside the mesopores is only partially occupied by the co-polymer and a residual pore volume is still available for guest inclusion.

Q loading (% Q) was evaluated by UV-vis spectrophotometry, after extraction with DMSO, and by thermogravimetric analysis (see Table 2).

In the case of the Q/MSN_{small} complex, the loading value as determined by TGA is in good agreement with the UV-Vis spectrophotometric result and it is considerably high (49.5% w/w). Q loading for the Q/copoly-MSN_{small} complex is also high, but it decreases significantly in comparison to the Q/MSN_{small} complex because of the hindrance of the grafted copolymer. Q loadings for the complexes prepared with MSN_{big} are lower, probably because the pore size is not the optimal one to host Q. The small discrepancy between loading values obtained by spectrophotometry and TGA are compatible with the accuracy of the methods.

The size of as-prepared MSNs suspended in ultrafiltered water and of their corresponding Q complexes was determined by DLS measurements. Comparing the results obtained for the copolymer-grafted nanoparticles with those of bare MSN_{small} and MSN_{big} (Table 3), a decrease in the average diameter is observed after functionalization, which indicates that poly(MPS-co-NIPAM) chains anchored to the MSNs prevents their aggregation. Concerning the Q/complexes, all of them show a mean diameter slightly higher than the corresponding bare matrices, thus suggesting that a fraction of the guest molecules is adsorbed on the external surface of the host nanoparticles.

The trend observed for the particle size is coherent with the changes in ζ potential value (Table 3). All samples show a negative ζ potential value, around -20 mV. For both MSNs a small decrease in negative charge is observed after copolymer grafting, confirming the presence of the copolymer attached to the silica surface. Since the change is small, the positive influence of grafting towards aggregation can be mainly explained with steric repulsion. Finally, the ζ potential average value is very similar in all Q complexes, irrespective of the starting material. This indicates that a small fraction of Q molecules is adsorbed on the external surface of the nanoparticles. Noticeably, the changes observed after Q inclusion are relatively larger in the samples prepared with MSN_{small}. Anyway, since in general these differences in ζ potential are small, it is not possible to draw definite conclusions about host/guest interactions in the different samples.

3.2. Biocompatibility of the silica matrices

The biocompatibility of MSN_{small} and MSN_{big}, either with or without grafted copolymer, was tested with the human keratinocyte cell line, HaCaT.

HaCaT cells were incubated with each sample at four different concentrations, in the range 0.291 – 17.5 ($\times 10^{-3}$) mg/mL, and cell proliferation was determined by SRB assay after 24 and 48 h (Fig. 2).

Both silica matrices up to the highest tested concentration (17.5×10^{-3} mg/mL) showed no toxicity after 24 h of cell growth, as such and after copolymer grafting. After 48 h, neither toxicity nor significant differences were observed at 0.291×10^{-3} and 2.91×10^{-3} mg/mL concentration, but at 8.75×10^{-3} and 17.5×10^{-3} mg/mL MSN_{big} caused a 30/40% loss in viability. No differences in cell viability were observed in the presence of copolymer-grafted MSN_{big}. The concentration 17.5×10^{-3} mg/mL MSN_{small} caused a small loss of viability (20%) only in the absence of the copolymer.

3.3. Testing of the properties of quercetin/MSNs complexes

3.3.1. Quercetin release tests

Initially, release tests were performed on the non-functionalized Q/MSNs complexes. As an example, in Fig. S1 the release profile of bare Q/MSN_{small} at 20 °C is reported. Namely, the flavonoid release from Q/MSN_{small} and Q/MSN_{big} complexes was found to be very fast and almost complete: after 5 min, released Q reached a value equal to 80%. This suggests that diffusion of the encapsulated molecules from inside the pores to outside does not significantly affect the kinetics of Q release, and that a consistent fraction of the active ingredient could be physisorbed on the external silica surface. Differently, with both copolymer-grafted MSNs, the release was not complete, indicating a stronger interaction with the host matrix (Fig. 3).

In order to verify the thermoresponsive behavior, $Q/copoly\text{-}MSN_{small}$ and $Q/copoly\text{-}MSN_{big}$ release profiles were monitored at 20 and 40 °C, that is below and above LCST, respectively (Fig. 3). In the case of small pores, a fast release was observed at both temperatures with a difference of 11.8% in the final amount of Q released. Reasonably, this gap is due to the copolymer response to the thermal *stimulus*. At temperatures above the LCST, in fact, the copolymer chains collapse, allowing the release of the flavonoid molecules immobilized within the mesopores. Concerning the sample with larger pores, a more gradual trend was observed, and the final difference in the release of Q between the two temperatures is

equal to 20.0%. These experimental evidences are in agreement with the physico-chemical characterization and suggest that in the matrices with small pores the active substance, although loaded in greater quantity, is predominantly physisorbed on the outer surface of the MSNs, while in the case of Q/copoly-MSN_{big} it can penetrate in depth into the mesopores also allowing an improved thermoresponsive behavior of the delivery system.

For this reason, only MSN_{big}, bare and functionalized, and the corresponding Q complexes were considered for further activity tests.

3.3.2. Antioxidant activity

The $DPPH^{\bullet}$ assay is widely employed in natural antioxidant studies being a simple and sensitive method. It is based on the ability of the antioxidant species to reduce (by electron transfer) the stable purple colored $DPPH^{\bullet}$ radical to the yellow colored diphenyl-picrylhydrazine. The antioxidant effect is proportional to the decrease in the absorption at 525 nm (purple color) and is reported as a radical scavenging activity.

Results obtained by the $DPPH^{\bullet}$ assay at RT revealed that the scavenging activity of Q, both free and immobilized, increased with its concentration. In particular, the antiradical effect of free Q ranged from 3.0 (±1.0)% to 40 (±1.0)% (see Fig. 4), meanwhile both complexes, Q/MSN_{big} and Q/copoly-MSN_{big}, showed an antiradical activity up to 72% and 53%, respectively. Considering that these experiments were carried out within 10 min at RT, and that according to the above reported release profiles about 90% and 50% of Q is released from Q/MSN_{big} and Q/copoly-MSN_{big} respectively, it is reasonable to hypothesize that the increased antioxidant effect, particularly pronounced in the case of the non-functionalized Q complex, might be due to the intrinsic radical scavenging capability of MSNs, recently discussed in the literature (Huang et al., 2010; Morry et al., 2015).

The metal chelating ability of an antioxidant agent can be considered as an adjuvant effect of the antioxidative effect. In fact, it has been demonstrated that reduced metal ions are active propagators of radical chains via hydroperoxide reduction to RO• (Prior et al., 2005). Thus, chelation of transition metal ions can inhibit ion-mediated oxidation of biomolecules.

Ferrozine can quantitatively form complexes with Fe^{2+}. In the presence of chelating agents, the complex formation is inhibited, leading to a decrease in the red color of the complexes between ferrous ions and ferrozine. The metal chelating ability is thus detected by measuring the absorbance of the corresponding Fe^{2+}-Ferrozine complex at 562 nm.

Results of the assay are plotted in Fig. 5 and show that for all the examined samples the metal-chelating effect is concentration dependent. The maximum activity, amounting to about 21%, was observed with free Q in a concentration of 50 µM. As regards the MSNs loaded with the flavonoid, there is a reduction in the activity compared to the free flavonoid, especially in the case of Q/copoly-MSN_{big} which shows a chelating capacity slightly lower than the corresponding non-functionalized sample. This is a reasonable result considering that the experiment was carried out at RT within 20 min, and according to the release profiles shown in Fig. 3, under these conditions about 60% of the flavonoid is released from Q/copoly-MSN_{big} and about 90% from Q/MSN_{big}. These results prove that the metal chelating effect occurs when the flavonoid is in the free form.

However, it is important to emphasize that this is a preliminary experiment and it should be considered only predictive of the maintenance of the antioxidant activity of the flavonoid included in the MSNs. It is performed in standard conditions of temperature and environment, thus, it does not replace the *ex vivo* activity tests on the skin, which will be partially addressed in the next section.

3.3.3. Ex vivo experiments on porcine skin

Ex vivo experiments performed employing vertical Franz diffusion cells and porcine skin membranes demonstrated that after 24 h from the application, no traces of Q were found in the receptor phase, independently from the tested sample (Q, Q/MSN_{big} and Q/copoly-MSN_{big}). This observation is consistent with our previous report (Sapino et al., 2015). The absence of transepidermal penetration of Q can be attributed both to the barrier properties of the *stratum corneum* and to the structure and physico-chemical characteristics of this flavonoid. Indeed, one of the reasons contributing to the inability of Q to penetrate the skin could be its poor lipophilicity and rather limited aqueous solubility [33]. However, although many scientists have focused their research efforts towards maximizing transdermal absorption of drugs [34], permeation of antioxidants such as Q is undesirable. Once the antioxidant has permeated into the systemic circulation, photoprotection is lost and the skin is susceptible to damage from sunlight. The accumulation in the *stratum corneum* and viable epidermis, which are the target layers of cosmetic active ingredients, is a precondition for the desirable protective effect of polyphenols against oxidative skin damage. In order to verify the feasibility of triggering the flavonoid release upon the skin contact, Q permeation and accumulation through porcine ear skin was studied by Franz cells running the experiment at 35 ± 1 °C that can be considered the average physiological temperature of the human skin in standard conditions. As receiving phase, a mixture of normal saline solution/ethanol (80/20 v/v) was chosen to ensure the complete solubility of Q. Ethanol was added to the receptor fluid due to its antimicrobial properties, in order to prevent skin deterioration during the experiment.

The formulation of the hydrogel medium used as donor phase was designed in order to ensure the incorporation of Q and the presence of an appropriate fraction of aqueous medium which allows the polymer to exhibit its characteristic coil-to-globule transition.

As reported in Fig. 6, modest skin accumulation levels were observed, in particular 4.68, 5.38 and 2.17 μg/cm^2 were measured for Q, Q/MSN_{big} and Q/copoly-MSN_{big}, respectively; notably, Q/MSN_{big} showed the greatest accumulation. This result suggests that probably MSN_{big} are more efficient in preserving Q

from degradative processes that occur after application on the skin. It is also evident that incorporation of Q in copoly-MSNs decreases skin accumulation as the amount of Q released from the nanoparticles to the gel is reduced. This limits the availability of the flavonoid to the *stratum corneum* whilst maintaining photoprotection. Possibly, higher accumulation values could be obtained for the copoly-MSN_{big} system by finely adjusting the LCST of the thermoresponsive copolymer according to the dermocosmetic formulation. Furthermore, it must be considered that this study is not fully exhaustive as it was conducted by static Franz cells over 24 h and using excised porcine skin membranes, so the follicular accumulation was not assessed.

4. Conclusions

MSNs have often been proposed to control the release of drugs and active compounds, but to our knowledge their use in cutaneous preparations has not been much documented so far. This work aims to realize an innovative delivery system (*i*) able to preserve the physico-chemical and biological properties of labile active ingredients of dermocosmetic interest until their release on the skin and (*ii*) able to trigger the release according to the temperature condition of the application site.

The antioxidant Q has been chosen as a model molecule, while copolymer-grafted MSNs with two different mesoporous sizes have been successfully prepared: both these systems displayed biocompatibility with immortalized human keratinocytes (HaCaT), particularly within 24 h. *In vitro* release profiles of Q/copoly-MSNs complexes demonstrated that thermoresponsive properties, more evident in the case of big pores, could be further improved by optimizing the size of the grafted chains. $DPPH^{\bullet}$ and Fe^{2+}-ferrozine assays demonstrated that the antioxidant efficacy of Q was maintained upon immobilization in the siliceous nanoparticles and it was likely improved by the intrinsic radical scavenging capability of the carrier.

Finally, *ex vivo* studies of Q accumulation and permeation through the skin from a hydrogel formulation underlined a certain role of the copolymer in hindering Q release and its interaction with the skin barrier. The research presented here obviously needs further studies, especially as for the relationship between surface properties of the copolymer-grafted MSNs and the physico-chemical characteristics of the overall formulation. However, based on these preliminary results, this innovative system can be considered as a promising and strategic approach to control the skin delivery of antioxidants and could be implemented to increase the efficacy of other active compounds.

Conflict of interest

The authors declare no conflict of interest in this work.

Acknowledgments

Compagnia di San Paolo – Italy and Università di Torino are gratefully acknowledged for funding Project ORTO114XNH through‘‘Bando per il finanziamento di progetti di ricerca di Ateneo – anno 2011’’. This research has been carried out also with the financial support of the Università di Torino [Fondi di Ricerca Locale (ex 60%) 2014, 2015]

References

Ambrogi, V., Perioli, L., Marmottini, F., Latterini, L., Rossi, C., Costantino, U., 2007. Mesoporous silicate MCM-41 containing organic ultraviolet ray absorbents: Preparation, photostability and in vitro release. J. Phys. Chem. Solids 68, 1173-1177.

Berlier, G., Gastaldi, L., Sapino, S., Miletto, I., Bottinelli, E., Chirio, D., Ugazio, E., 2013a. MCM-41 as a useful vector for rutin topical formulations: Synthesis, characterization and testing. Int. J. Pharm. 457, 177-186.

Berlier, G., Gastaldi, L., Ugazio, E., Miletto, I., Iliade, P., Sapino, S., 2013b. Stabilization of quercetin flavonoid in MCM-41 mesoporous silica: positive effect of surface functionalization. J. Colloid Interf. Sci. 393, 109-118.

Brunella, V., Jadhav, S.A., Miletto, I., Berlier, G., Ugazio, E., Sapino, S., Scalarone, D., 2016. Hybrid drug carriers with temperature-controlled on-off release: A simple and reliable synthesis of PNIPAM-functionalized mesoporous silica nanoparticles. React. Funct. Polym. 98, 31-37.

Ehren, J.L., Maher, P., 2013. Concurrent regulation of the transcription factors Nrf2 and ATF4 mediates the enhancement of glutathione levels by the flavonoid fisetin. Biochem. Pharmacol. 85, 1816-1826.

Gandhi, A., Paul, A., Sen, S.O., Sen, K.K., 2015. Studies on thermoresponsive polymers: Phase behaviour, drug delivery and biomedical applications. Asian J. Pharm. Sci. 10, 99-107.

Gastaldi, L., Ugazio, E., Sapino, S., Iliade, P., Miletto, I., Berlier, G., 2012. Mesoporous silica as a carrier for topical application: the Trolox case study. Phys. Chem. Chem. Phys. 14, 11318-11326.

Huang, X.L., Zhuang, J., Teng, X., Li, L.L., Chen, D., Yan, X.Y., Tang, F.Q., 2010. The promotion of human malignant melanoma growth by mesoporous silica nanoparticles through decreased reactive oxygen species. Biomaterials 31, 6142-6153.

Jadhav, S.A., Miletto, I., Brunella, V., Berlier, G., Scalarone, D., 2015. Controlled post-synthesis grafting of thermoresponsive poly(N-isopropylacrylamide) on mesoporous silica nanoparticles. Polym. Advan. Technol. 26, 1070-1075.

Kim, H.W., Gwak, H.S., Chun, I.K., 2004. The effect of vehicles and pressure sensitive adhesives on the percutaneous absorption of quercetin through the hairless mouse skin. Arch. Pharm. Res. 27, 763-768.

Kresge, C.T., Leonowicz, M.E., Roth, W.J., Vartuli, J.C., Beck, J.S., 1992. Ordered mesoporous molecular-sieves synthesized by a liquid-crystal template mechanism. Nature 359, 710-712.

Kumar, S., Pandey, A.K., 2013. Chemistry and Biological Activities of Flavonoids: An Overview. Sci. World J. 2013, 1-16, doi.org/10.1155/2013/162750.

Li, B., Konecke, S., Harich, K., Wegiel, L., Taylor, L.S., Edgar, K.J., 2013. Solid dispersion of quercetin in cellulose derivative matrices influences both solubility and stability. Carbohyd. Polym. 92, 2033-2040.

Maalik, A., Khan, F.A., Mumtaz, A., Mehmood, A., Azhar, S., Atif, M., Karim, S., Altaf, Y., Tariq, I., 2014. Pharmacological Applications of Quercetin and its Derivatives: A Short Review. Trop. J. Pharm. Res. 13, 1561-1566.

Middleton, E., Kandaswami, C., Theoharides, T., 2000. The effects of plant flavonoids on mammalian cells: implications for inflammation, heart disease, and cancer. Pharm. Rev. 52, 673–751.

Miyake, T., Shibamoto, T., 1997. Antioxidative activities of natural compounds found in plants. J. Agric. Food Chem. 45, 1819-1822.

Morry, J., Ngamcherdtrakul, W., Gu, S.D., Goodyear, S.M., Castro, D.J., Reda, M.M., Sangvanich, T., Yantasee, W., 2015. Dermal delivery of HSP47 siRNA with NOX4-modulating mesoporous silica-based nanoparticles for treating fibrosis Biomaterials 66, 41-52.

Natalia, F., Stoychev, G., Puretskiy, N., Leonid, I., Volodkin, D., 2015. Porous thermo-responsive pNIPAM microgels. Eur. Polym. J. 68, 650-656.

Prior, R.L., Wu, X., Schaich, K., 2005. Standardized methods for the determination of antioxidant capacity and phenolics in foods and dietary supplements. J. Agr. Food Chem. 53, 4290-4302.

Rabe, E., Agus, G.B., Roztocil, K., 2015. Analysis of the effects of micronized purified flavonoid fraction versus placebo on symptoms and quality of life in patients suffering from chronic venous disease: from a prospective randomized trial. Int. Angiol. 34, 428-436.

Ribeiro, D., Freitas, M., Lima, J., Fernandes, E., 2015. Proinflammatory Pathways: The Modulation by Flavonoids. Med. Res. Rev. 35, 877-936.

Roubalova, L., Purchartova, K., Papouskova, B., Vacek, J., Kren, V., Ulrichova, J., Vrba, J., 2015. Sulfation modulates the cell uptake, antiradical activity and biological effects of flavonoids in vitro: An examination of quercetin, isoquercitrin and taxifolin. Bioorgan. Med. Chem. 23, 5402-5409.

Saija, A., Tomaino, A., Trombetta, D., Giacchi, M., De Pasquale, A., Bonina, F., 1998. Influence of different penetration enhancers on in vitro skin permeation and in vivo photoprotective effect of flavonoids. Int. J. Pharm. 175, 85-94.

Sapino, S., Ugazio, E., Gastaldi, L., Miletto, I., Berlier, G., Zonari, D., Oliaro-Bosso, S., 2015. Mesoporous silica as topical nanocarriers for quercetin: characterization and in vitro studies. Eur. J. Pharm. Biopharm. 89, 116-125.

Scallon, C., Bell-Syer, S.E.M., Aziz, Z., 2013. Flavonoids for treating venous leg ulcers. Cochrane Db. Syst. Rev. 5, 1-16, DOI: 10.1002/14651858.CD006477.pub2.

Schild, H.G., 1992. Poly (*N*-isopropylacrylamide) - experiment, theory and application, Prog. Polym. Sci. 17, 163-249.

Siasos, G., Tousoulis, D., Tsigkou, V., Kokkou, E., Oikonomou, E., Vavuranakis, M., Basdra, E.K., Papavassiliou, A.G., Stefanadis, C., 2013. Flavonoids in Atherosclerosis: An Overview of Their Mechanisms of Action. Curr. Med. Chem. 20, 2641-2660.

Skehan, P., Storeng, R., Scudiero, D., Monks, A., McMahon, J., Vistica, D., Warren, J.T., Bokesch, H., Kenney, S., Boyd, M.R., 1990. New colorimetric cytotoxicity assay for anticancer-drug screening. J. Natl. Cancer I. 82, 1107-1112.

Vichai, V., Kirtikara, K., 2006. Sulforhodamine B colorimetric assay for cytotoxicity screening. Nat. Protoc. 1, 1112-1116.

Wang, S., 2009. Ordered mesoporous materials for drug delivery. Micropor. Mesopor. Mat. 117, 1-9.

Werner, I., Guo, F.W., Kiessling, A.H., Juengel, E., Relja, B., Lamm, P., Stock, U.A., Moritz, A., Beiras-Fernandez, A., 2015. Treatment of endothelial cell with flavonoids modulates transendothelial leukocyte migration. Phlebology 30, 405-411.

Table 1. Specific surface area (SSA), pore volume, mean pore diameter of bare and copolymer-grafted MSNs, measured by gas-volumetric analysis.

Sample	SSA (m^2/g)	Pore volume (cm^3/g)	Mean pore diameter (Å)	Ref.
MSN_{small}	1228	1.45	35	[25]
Copoly-MSN_{small}	805	0.40	31	[25]
MSN_{big}	1017	2.42	49	[28]
Copoly-MSN_{big}	876	1.60	46	[28]

Table 2. Data from thermogravimetric analysis (percentage weight loss) and from UV–Vis spectrophotometric analysis (percentage of loading, % wt Q).

Samples	**Q loading by TGA (% wt)**	**Q loading by UV-Vis (% wt)**
Q/MSN$_{small}$	49.5	49.5
Q/copoly-MSN$_{small}$	32.4	39.4
Q/MSN$_{big}$	37.0	33.2
Q/copoly-MSN$_{big}$	33.5	26.4

Table 3. Mean particle size and ζ potential value of MSNs and their Q complexes, suspended in ultra-filtered water.

Sample	Average diameter (nm)	Average ζ potential (mV)
MSN_{small}	227 (± 7)	-26.8 ± 0.6
MSN_{big}	188 (± 20)	-20.7 ± 1.0
Copoly-MSN_{small}	106 (± 5)	-29.3 ± 0.4
Copoly-MSN_{big}	152 (± 6)	-24.3 ± 1.1
Q/MSN_{small}	351 (± 32)	-19.0 ± 0.8
Q/MSN_{big}	393 (± 22)	-20.3 ± 0.7
Q/copoly-MSN_{small}	328 (± 33)	-20.6 ± 0.7
Q/copoly-MSN_{big}	200 (± 19)	-21.3 ± 0.5

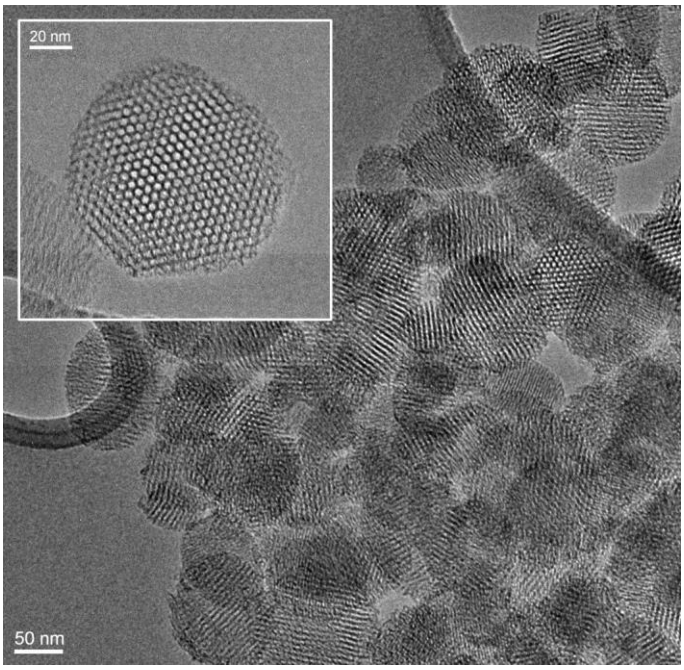

Figure 1. HRTEM images of MSN_{big}.

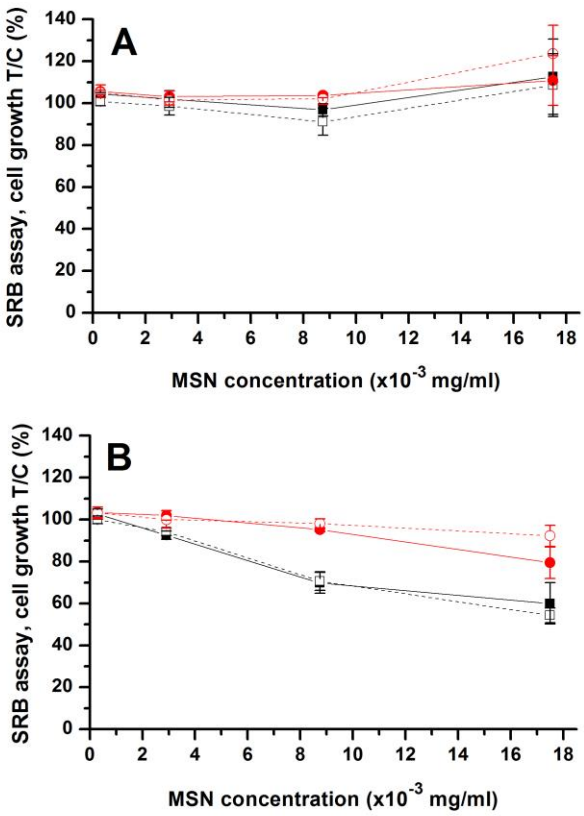

Figure 2. Effect of MSN_{big} (filled squares, black solid line), copoly-MSN_{big} (empty squares, black dashed line), MSN_{small} (filled circles, red solid line), copoly-MSN_{small} (empty circles, red dashed line) on HaCaT cell proliferation by SRB assay. Cells were incubated with the silica nanoparticles at different concentrations for 24 h (**A**) or 48 h (**B**). Cell growth is expressed as % T/C (mean OD of treated cells/mean of control cells × 100). Values are mean ± SD (n=3 wells/condition) of two independent experiments (for the interpretation of the colour code, the reader should refer to the web version of the article).

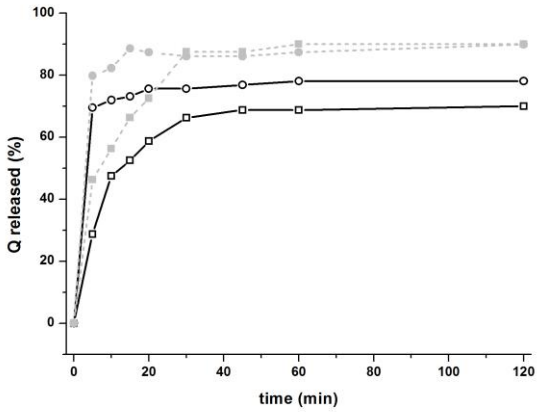

Figure 3. Q release profiles at 20 °C (empty symbols, black solid lines) and 40 °C (filled symbols, grey dashed line) from Q/copoly-MSN_{small} (circles) and Q/copoly-MSN_{big} (squares).

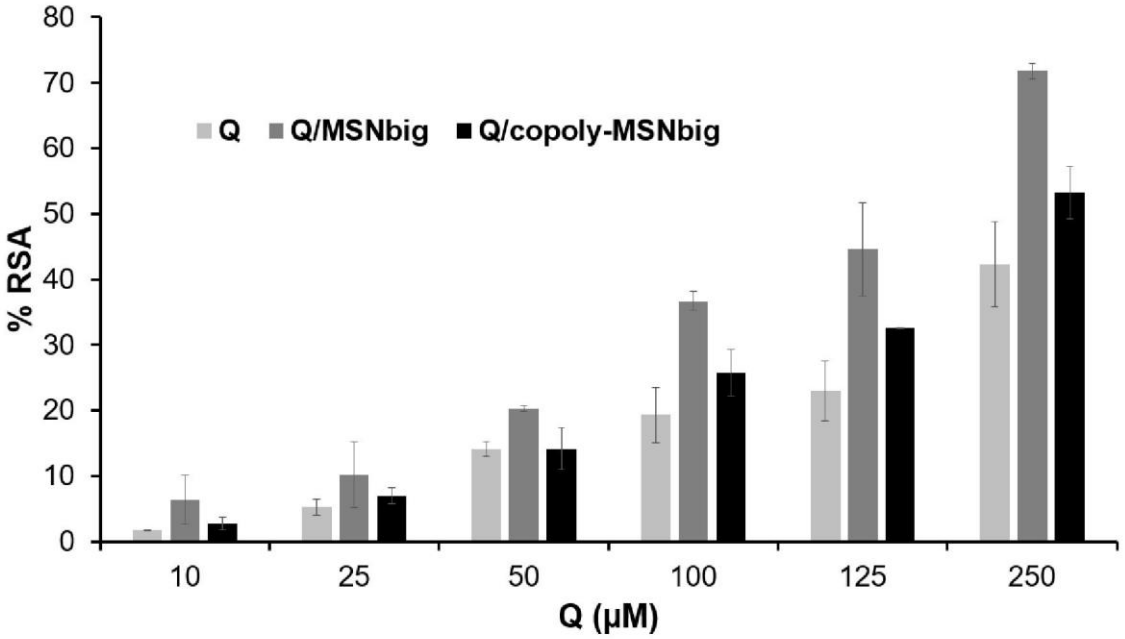

Figure 4. Antiradical activity (% RSA) towards DPPH$^{\bullet}$ of increasing concentration of Q, free or immobilized. Each bar represents the mean ± SD obtained in three independent experiments.

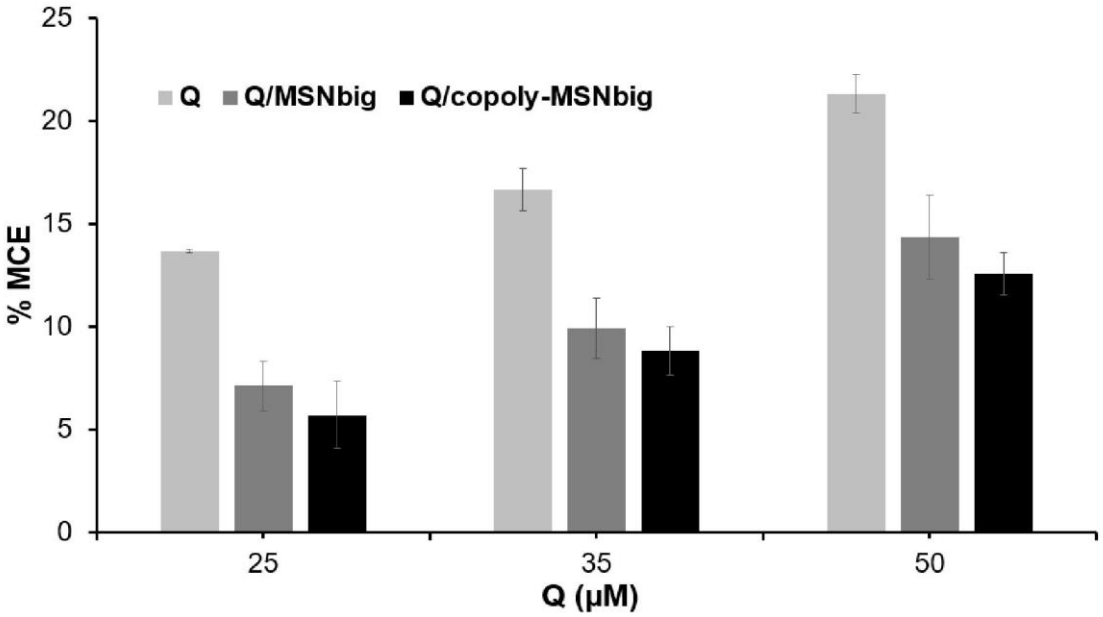

Figure 5. Metal chelating effect (% MCE) towards Fe^{2+} of increasing concentration of Q, free or immobilized. Each bar represents the mean ± SD obtained in three independent experiments.

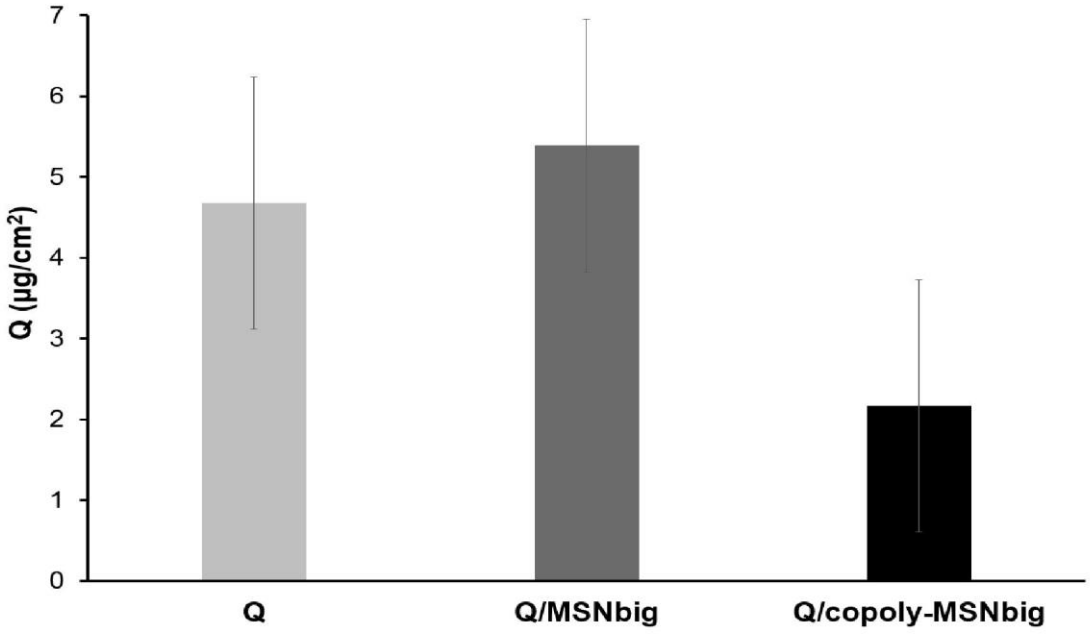

Figure 6. Amounts of Q retained by porcine skin (at 35 ± 1 °C), 24 h after application of the hydrogel containing Q, Q/MSN_{big} or Q/copoly-MSN_{big}. Each bar represents the mean ± SD obtained in three independent experiments.

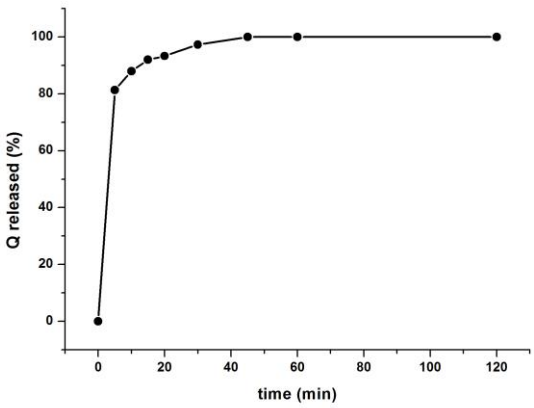

Fig. S1. Q release profiles at 20 °C from Q/MSN_{small}.